UCL

Design and first results of a scintillator-based, integrated mode proton imaging detector using 2D lateral projections

Ion Imaging Workshop - 2022

Ryan Fullarton[1], Mikaël Simmard[1], Daniel Robertson[2], Alison Toltz[3], Vasilis Rompokos[3], Sam Beddar[4], Charles-Antoine Collins Fekete[1]

Ryan.fullarton.20@ucl.ac.uk

(1) Medical Physics & Biomedical Engineering - University College London
(2) Medical Physics, Department of Radiation Oncology, Mayo Clinic Arizona.
(3) Proton Physics Group, Radiotherapy Physics, University College London Hospitals NHS Foundation Trust
(4) Department of Radiation Physics, University of Texas MD Anderson Cancer Center.

PRT MAYO CLINIC University College London Hospitals NHS Foundation Trust THE UNIVERSITY OF TEXAS MD Anderson Cancer Center Making Cancer History CANCER RESEARCH UK RADNET CITY OF LONDON

Aims

- **Fast low-dose proton imaging for use in positioning, motion management and online adaption**

- Single-event proton imaging
  - High quality
  - Low dose
  - Slow

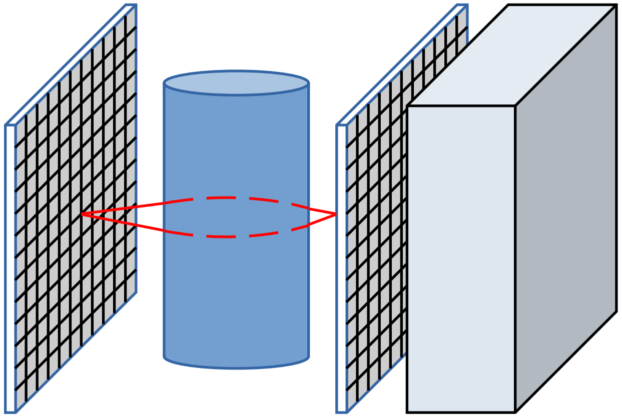

- Integrated proton imaging
  - Quality?
  - Low dose?
  - Fast(er)

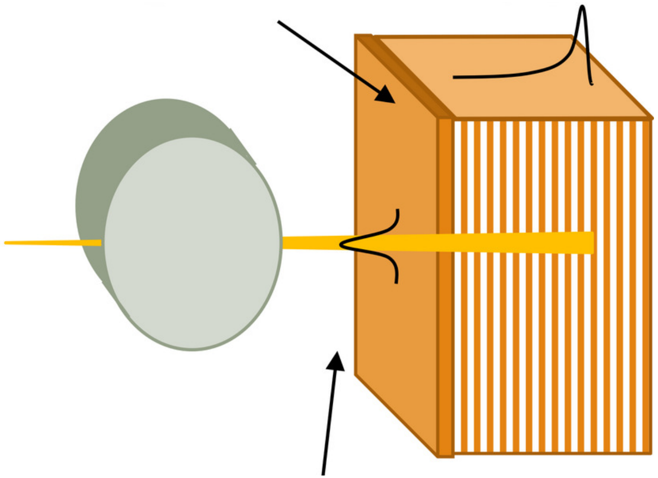

Background – Detector Concept

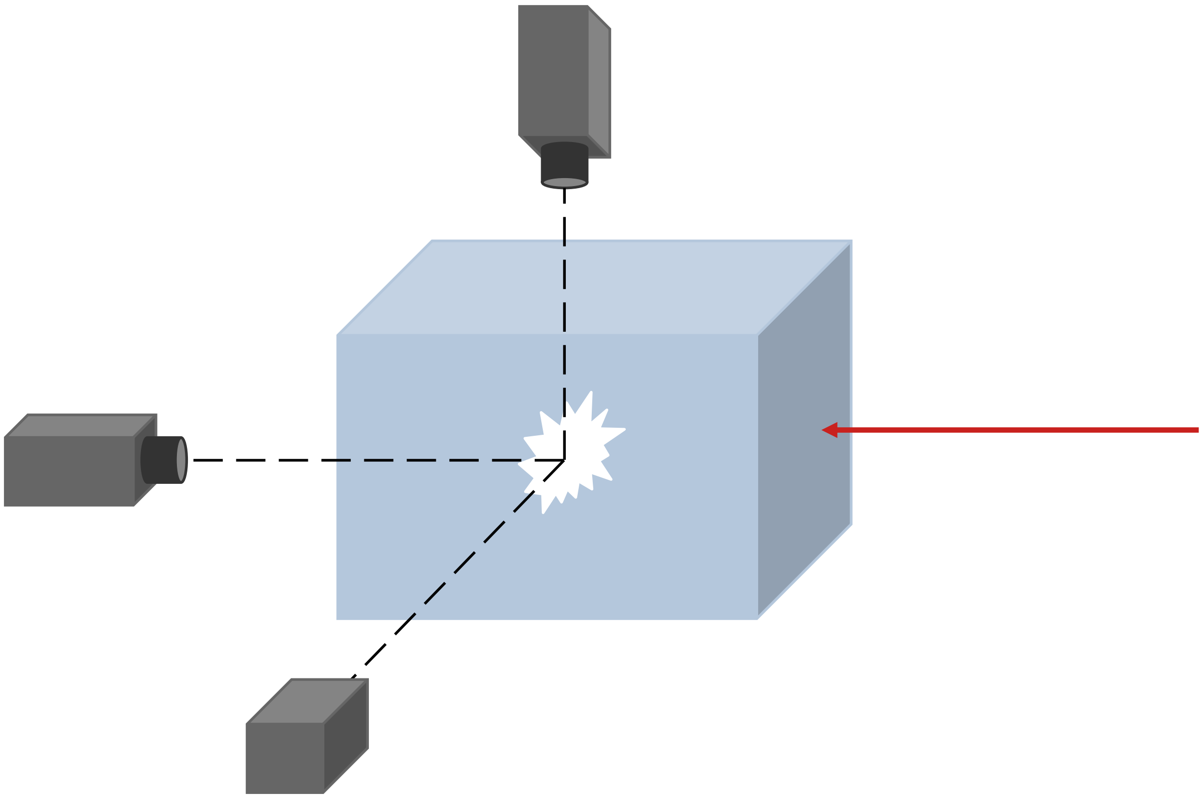

Concept – Testing in Simulation

- First validation in Geat4 V4.12
  - Pencil beams, 3mm spot size, 2mrd divergence, 3 mm spacing, 10^7 particles per pencil beam
  - 30 x 30 x30 cm^3 scintillator (EJ260)
  - XCAT phantom – mapped to ICRU materials

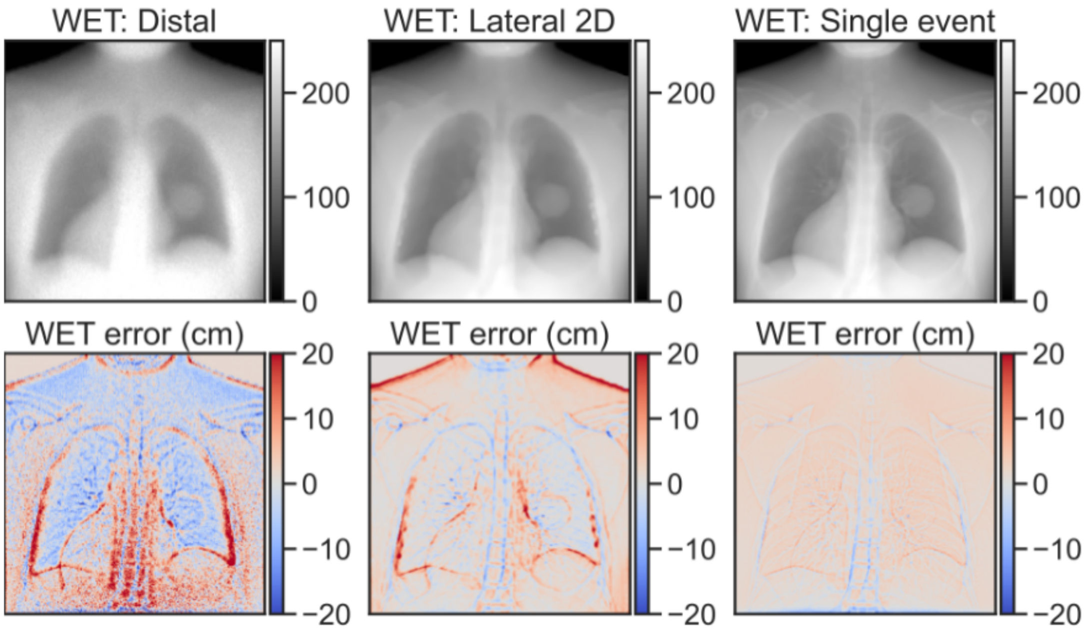

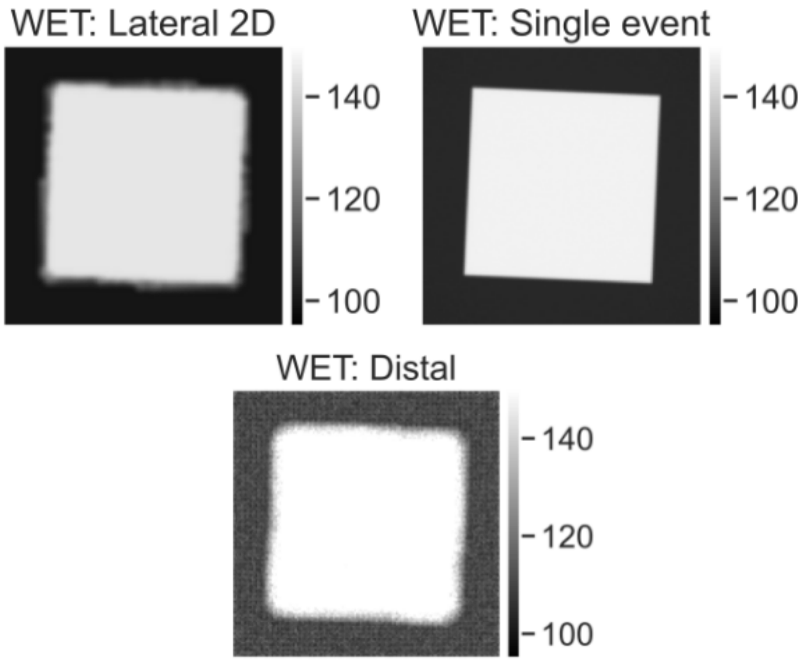

Background – Detector Design

UCL

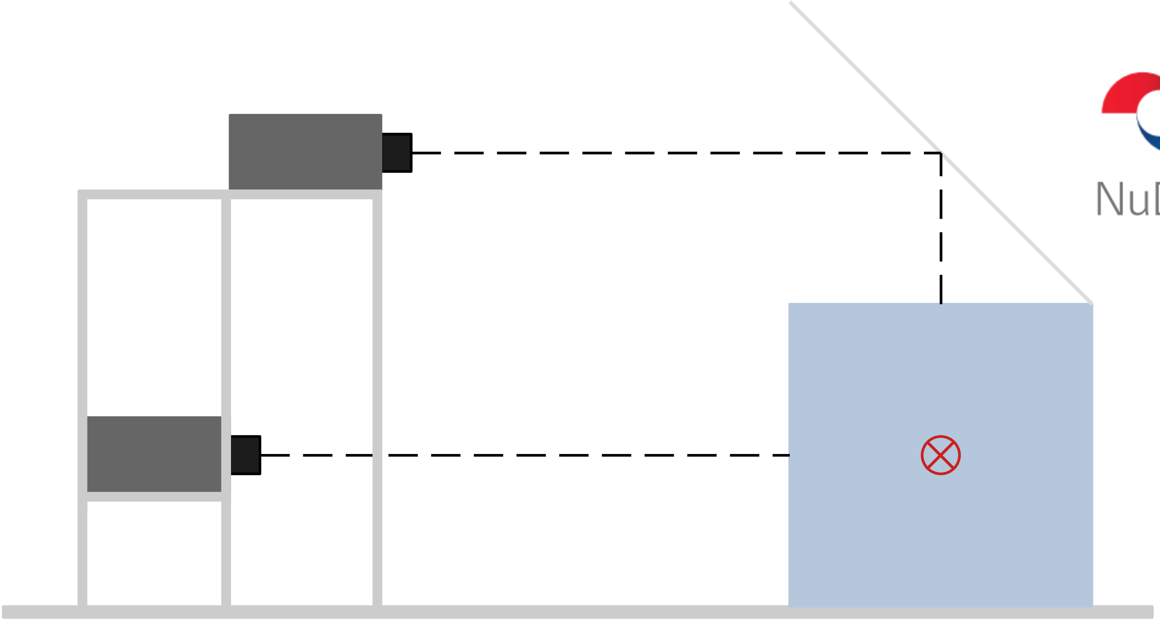

NUVIATECH INSTRUMENTS

NuDET PLASTIC Plastic Scintillation Detectors

THORLABS

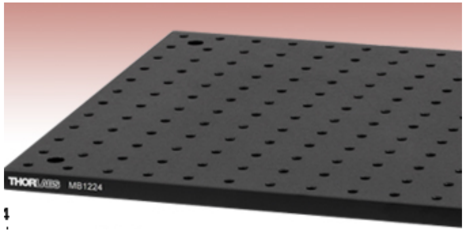

Reconstruction - 2 x 2D lateral views

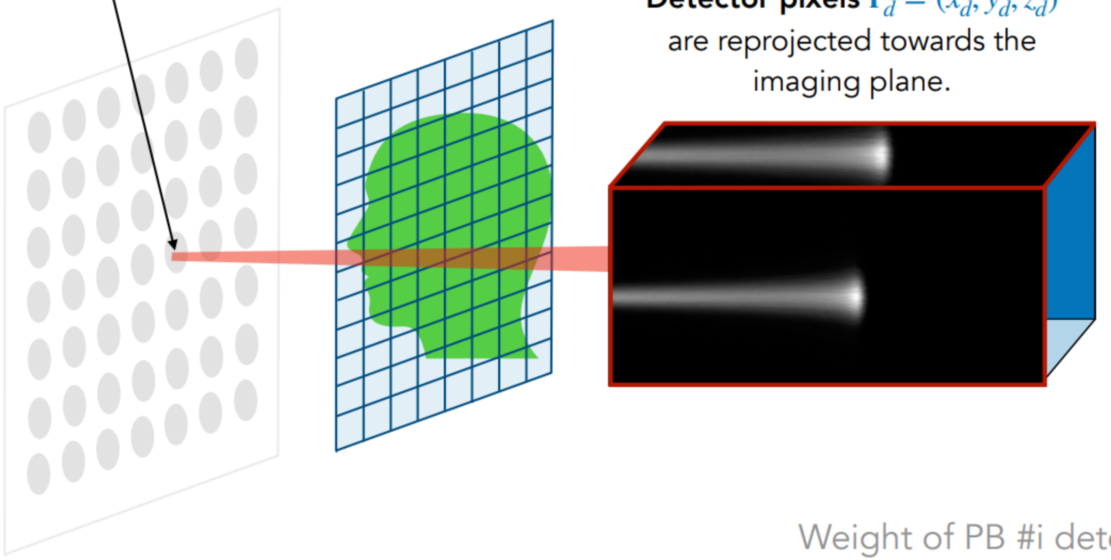

$$g(\mathbf{r}_k) = \frac{\sum_{i=1}^{n_{PB}} w_i(\mathbf{r}_k, \mathbf{r}_d) \frac{N_i(\mathbf{r}_d)}{N_{i,\mathrm{tot}}} \mathrm{WET}_i(\mathbf{r}_d)}{\sum_{i=1}^{n_{PB}} w_i(\mathbf{r}_k, \mathbf{r}_d) \frac{N_i(\mathbf{r}_d)}{N_{i,\mathrm{tot}}}}$$

Radiograph

Sum over all PBs

WET of PB #i at depth $\mathbf{r}_d$

Weight of PB #i detected at $\mathbf{r}_d$ for imaging pixel $\mathbf{r}_k$.

Fraction of **protons** that deposit energy at $\mathbf{r}_d$ (filters out low signal)

- $w_i(\mathbf{r}_k, \mathbf{r}_d)$: **physics-based** calculation (multiple Coloumb scattering based on Fermi-Eyges theory) that depends on PB and scintillator properties (spot size, angular divergence, emittance, scintillator material) and various geometric assumptions.

- **Nudet Plastic Scintillator**
  - 20 cm x 20 cm x 25cm polystyrene based scintillator
  - Emits light with a λ= 430 nm with an output 56% relative to anthracene
  - Decay time - 2.5ns, density - 1.03 g/cm
  - Sanded on 3 sides and painted with Culture Hustle Black 2.0 (absorbs 96% of visible light) to reduce internal reflections

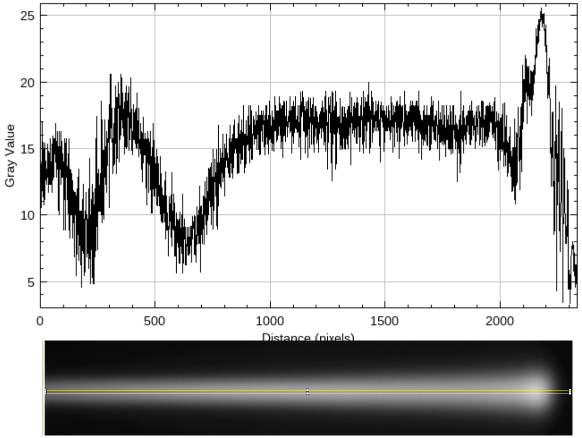

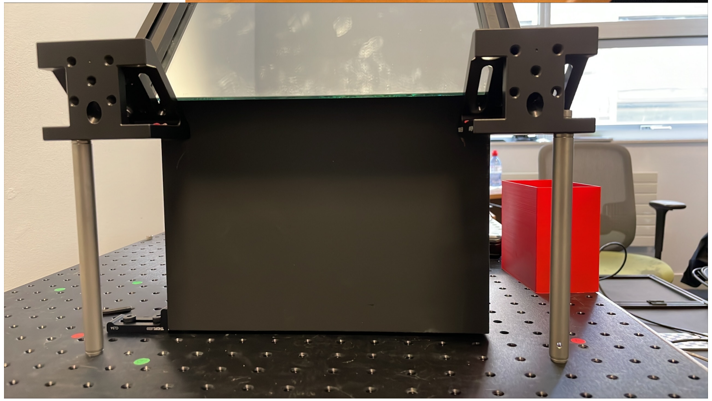

Light Acquisition

- **2 x FLIR Oryx 10GigE 51s5m monochrome cameras**
  - 2 x 5MP LM6HC lenses
    - f = 6 mm
    - Focused on central plane of the scintillator
    - Working distance 50 mm
    - 80 cm x 60 cm
  - 2x binning and cropped to give 25 cm x 20 cm FOV at front face of the scintillator
  - 0.4 mm – 0.6 mm resolution
  - 608 x 468 pixels ROI for faster readout
  - 350FPS acqusition

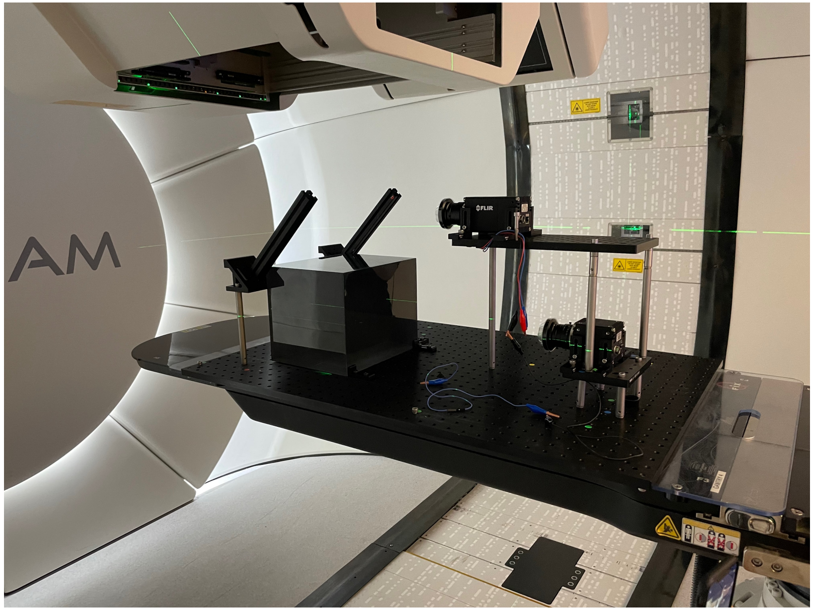

Acquisition Triggering

- **Treatment machine signals**
  - Accurately represent beam delivery
  - As fast as the beam delivers
  - Requires manufacturer permission
- **Software – Image analysis**
  - Based on what the camera sees
  - As fast as the camera can aquire
  - Requires as much time between beams as beam delivery
  - Requires set ‘Background’ and threshold
- **Hardware – Light output**
  - As fast as the response time of the electronics
  - Can trigger of different points in the signal
  - Additional testing

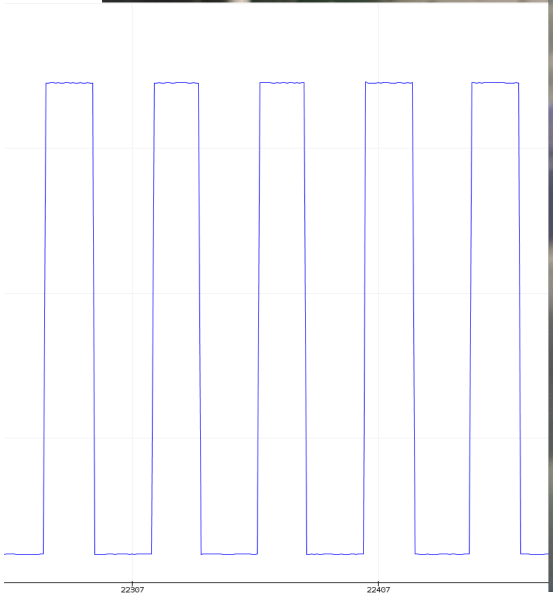

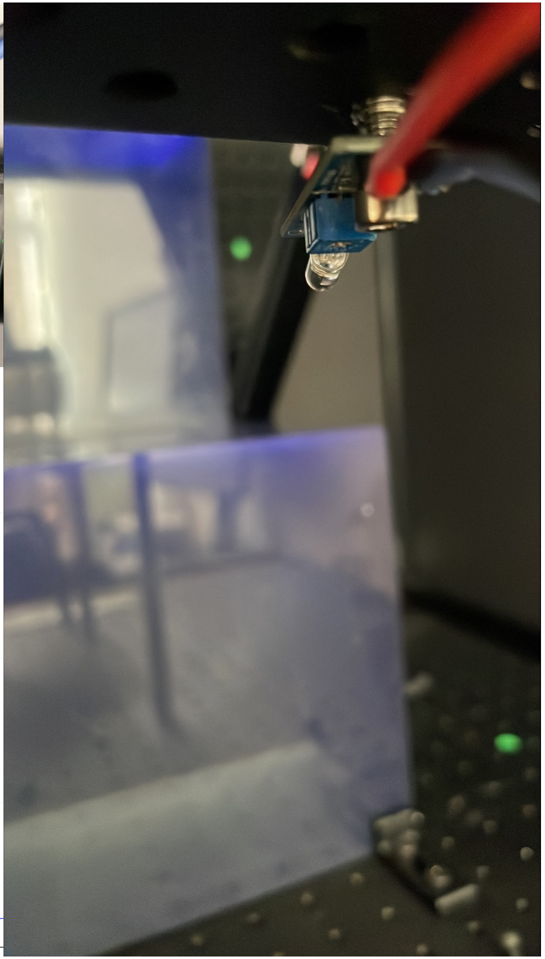

Top

Lateral

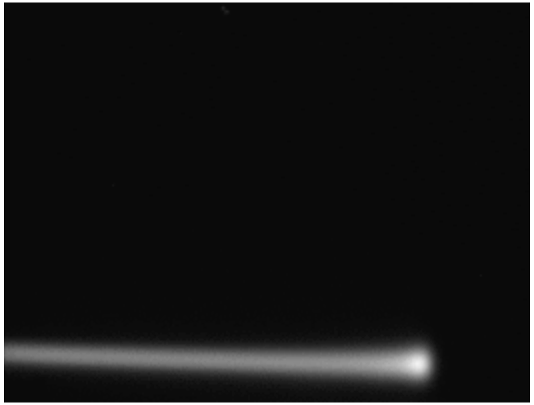

Range accuracy

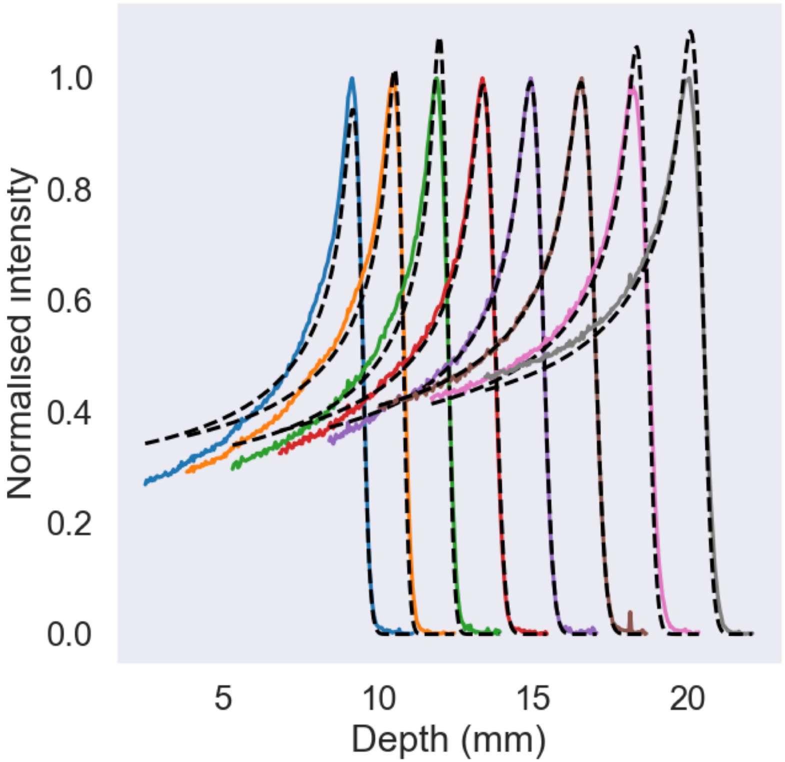

Energy (MeV	Range error (mm)
110	-3.3
120	-1.4
130	0.1
140	1.7
150	4.4
160	6.2
170	8.3
180	11.5
MAE	4.6

R_0 determined through a fit of a quenched Bragg Peak (Kelleter & Jolly, 2020)

Requires Correction for optical effects! (Robertson et al., 2014)

Lens based optical corrections

- **Vignetting**
  - Usually described by a $\cos^4$ function (Ray, 1994)
  - Characterized by white light field/camera parameters
  - Less light at extremities of the lenses

$$V_{i,j} = \cos^4(\theta_{i,j}) = \frac{a^4}{(a^2 + d_{i,j}^2)^2}$$

Optical Vignetting

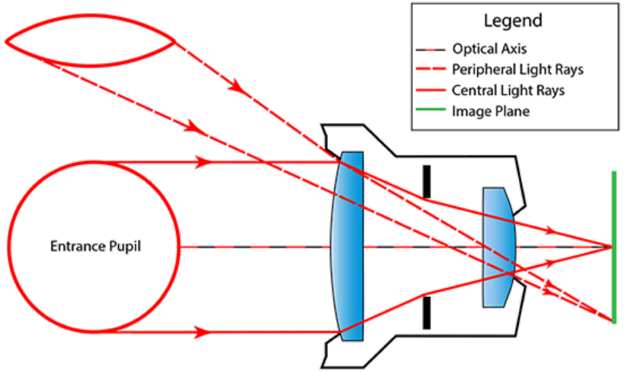

- **Distortion**
  - Causes by zoom lenses aberrations
  - Use vanishing lines to find the focal point of the camera
  - Second-order symmetric radial distortion mode (Zhang *et al.*, 1999)
  - Can be measured through mapping distances known in object and image space

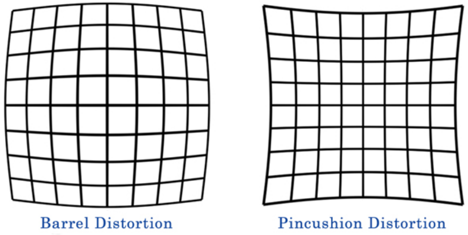

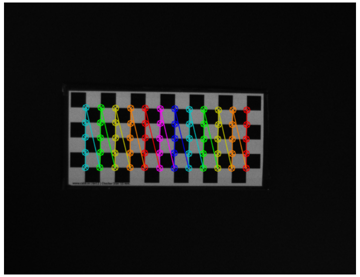

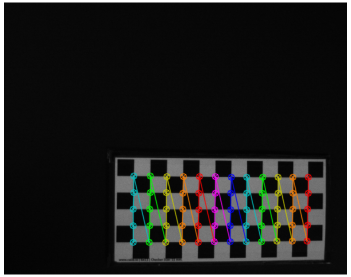

Lens based optical corrections

Uncorrected

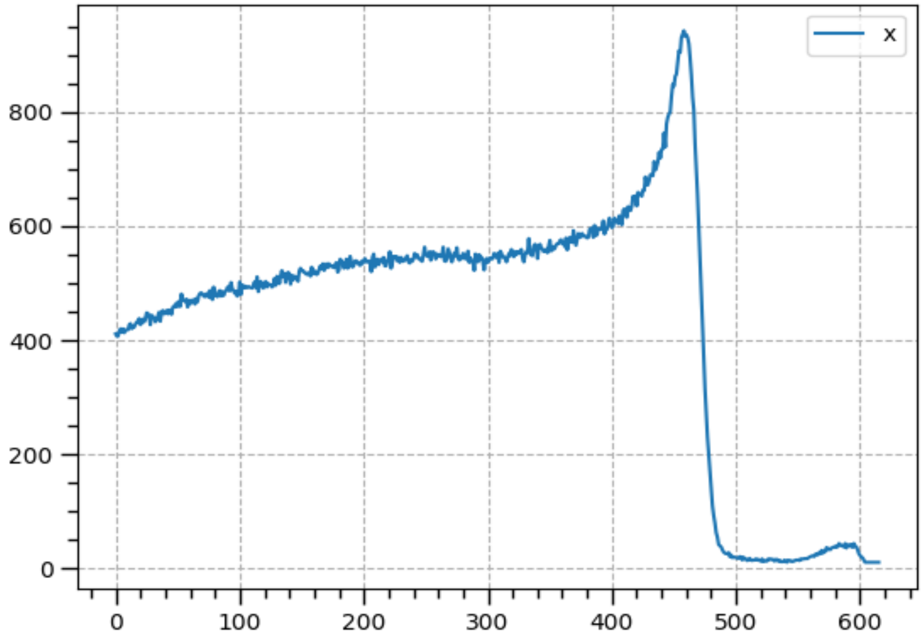

Vignetting Corrected

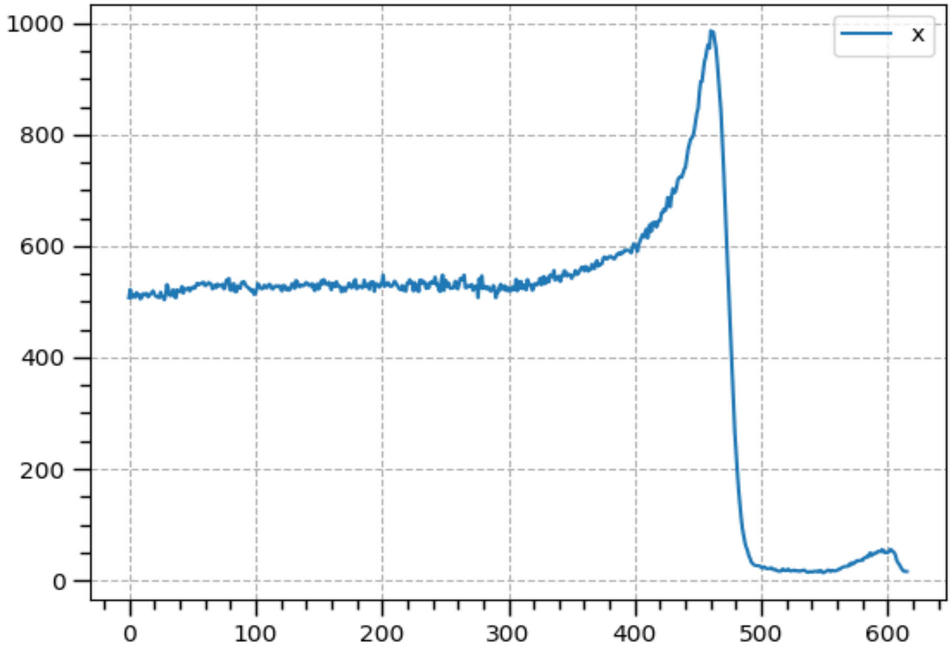

Geometry – Perspective & Refraction

The further away a beam is the further into the image its position appears

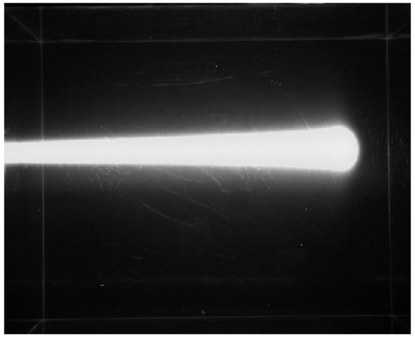

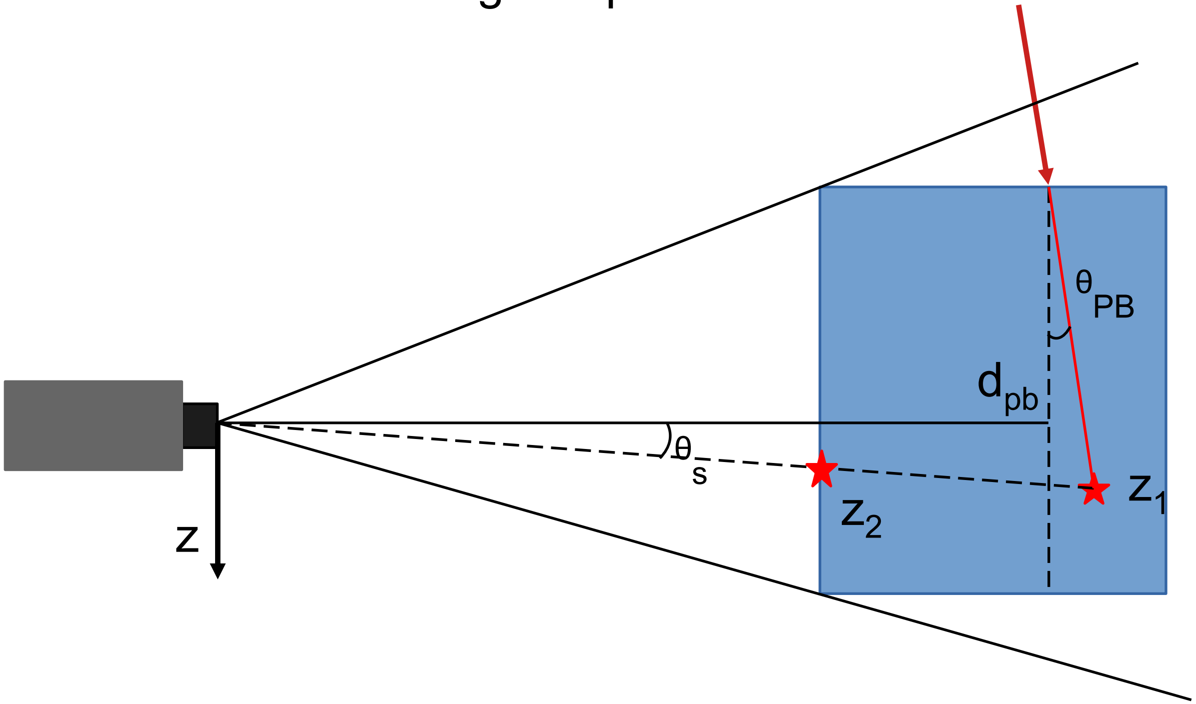

$$\frac{z_2}{d_s} = \frac{z_1}{d_{PB} + z_1 \tan \theta_{PB}}$$

Geometry – Perspective & Refraction

The further away a beam is the further into the image its position appears

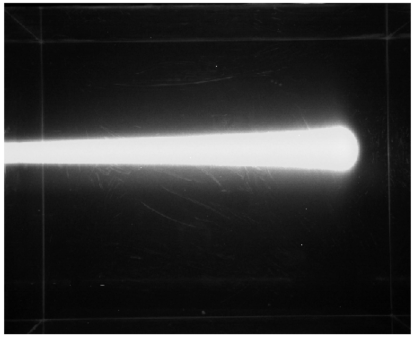

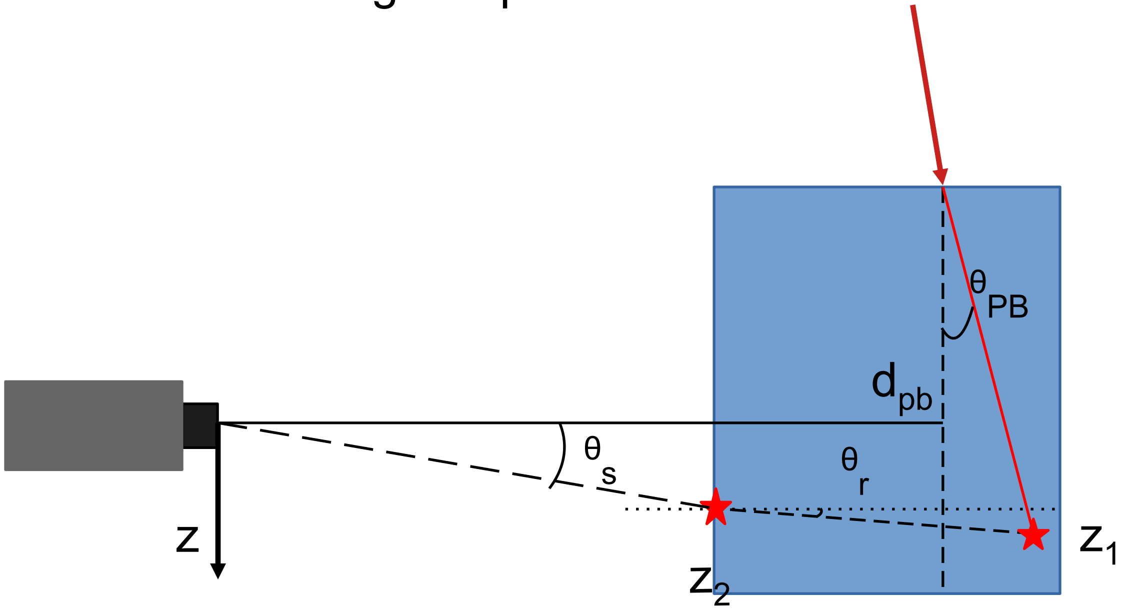

$$\theta_r = \sin^{-1}\left(\frac{1}{n_r}\sin\theta_s\right)$$

$$\tan\theta_r = \frac{z_1 - z_2}{d_{PB} + z_1 \sin\theta_{PB} - d_s}$$

Optical corrected range accuracy

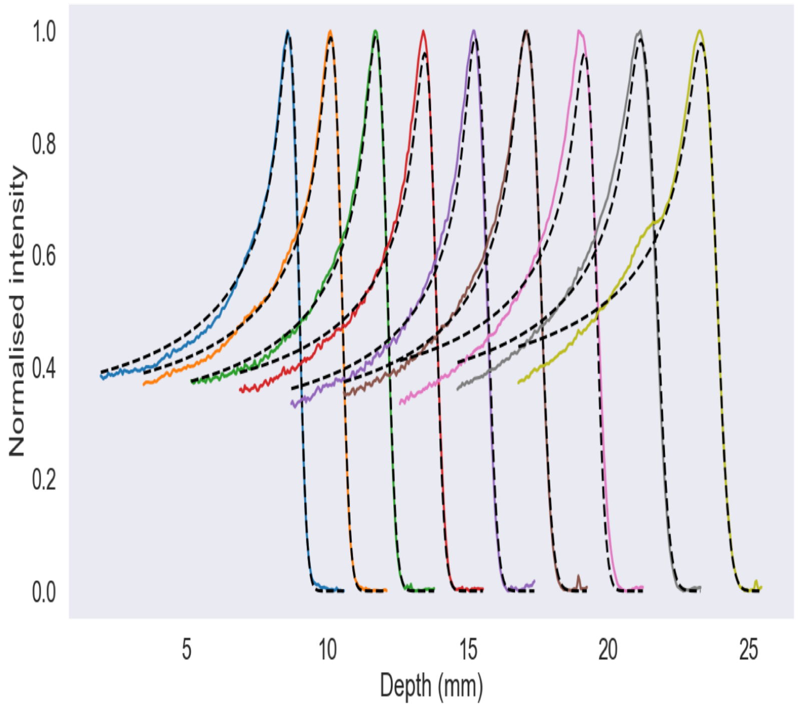

Energy (MeV	Range error (mm)
110	1.6
120	1.5
130	1.5
140	0.9
150	1.0
160	0.7
170	-0.1
180	-0.1
190	1.0
MAE	0.9

Optical corrected spot positions

Spot positions from imaging acquisition with a similar detector at Mayo Clinic Arizona by Dr. Daniel Robertson & Dr. Mikaël Simard

x TPS*
o lateral views

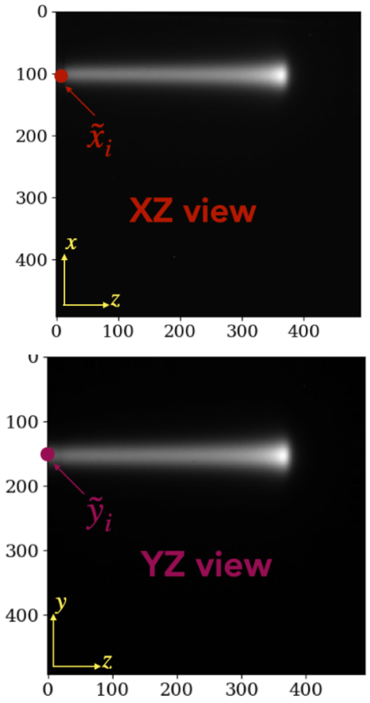

No corrections: images will appear warped

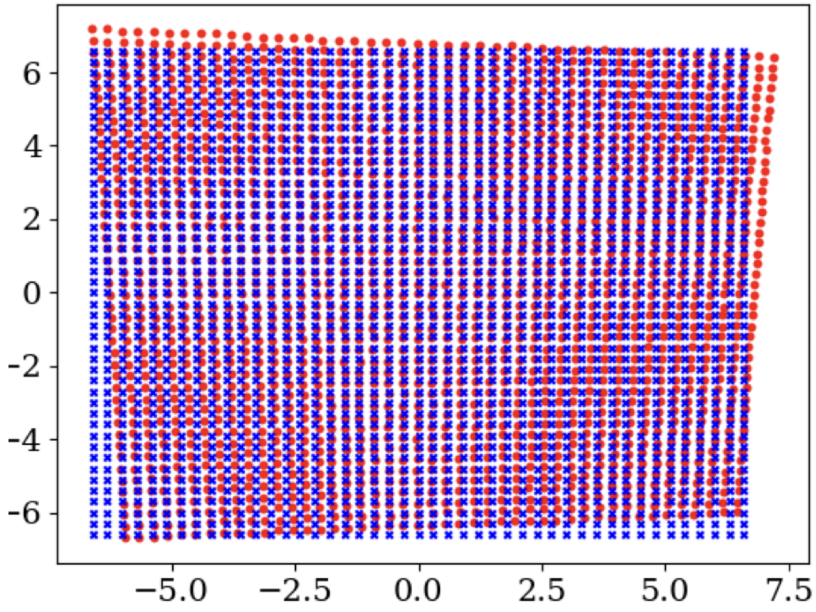

Corrections: most issues solved, slight issues to be addressed with upcoming distortion corrections

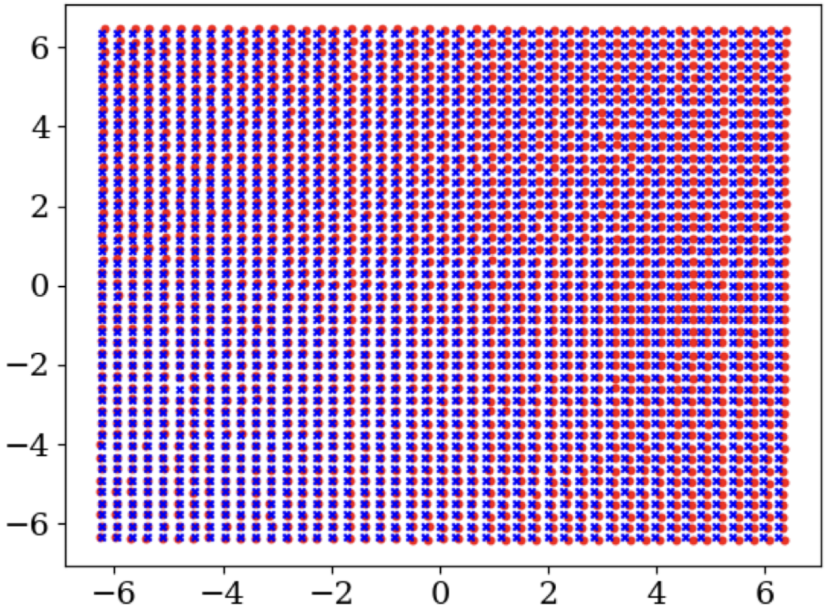

Imaging Dose

- Dose measurements for similar imaging system at Mayo Clinic Arizona by Dr. Daniel Robertson
  - Dose measured with ionisation chamber at 5cm depth in a 15x15 cm acrylic block
  - Imaging dose is currently limited by acquisition speed
  - Data shows that for low doses range accuracy is maintained

- The 1D approach (**integrate 2D images)** is also robust to low dose; the position of the Bragg peak does not change with MU.

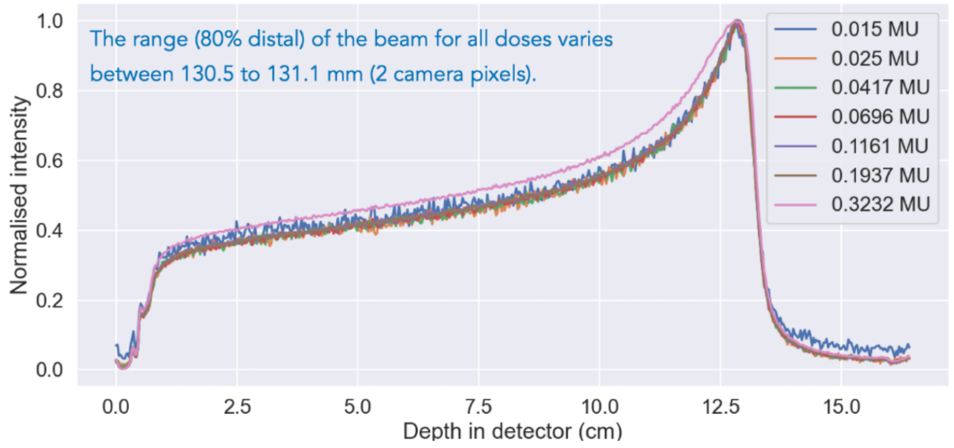

135.6 MeV

Spot Spacing	2 mm	3 mm	4 mm	5 mm
Dose during measurements (cGy)	515.2	257.2	128.9	82.4
Dose at minimum MU/spot (cGy)	6.2	2.8	1.5	1.0

189 MeV

Spot Spacing	2 mm	3 mm	4 mm
Dose during measurements (cGy)	475.9	226.8	238.4
Dose at minimum MU/spot (cGy)	5.7	2.5	1.4

Results indicate that dose may be **reduced** by a **factor** of **at least 10** without an important impact on image quality.

Imaging Dose

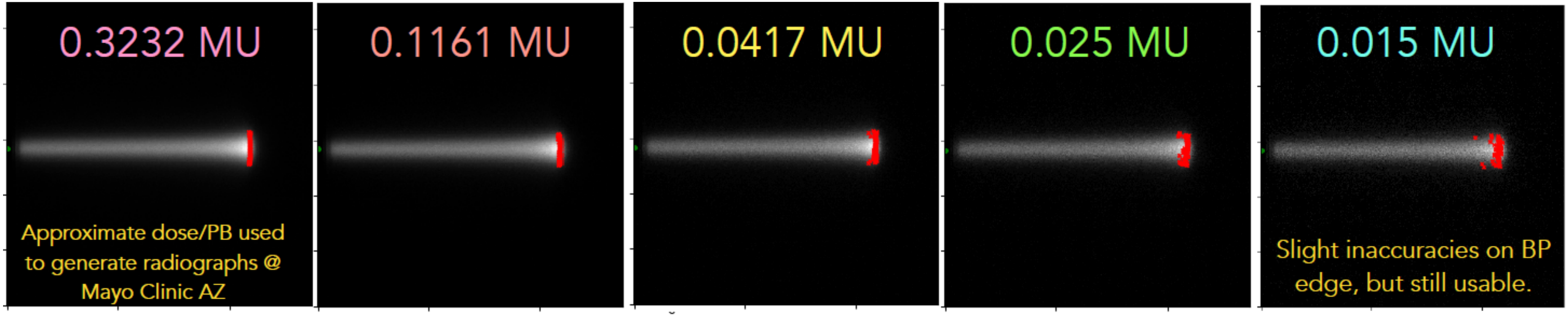

Conclusion

- Potential for producing Radiographs
  - Fast
  - Reasonable Quality
  - Reasonable dose

Top

Lateral

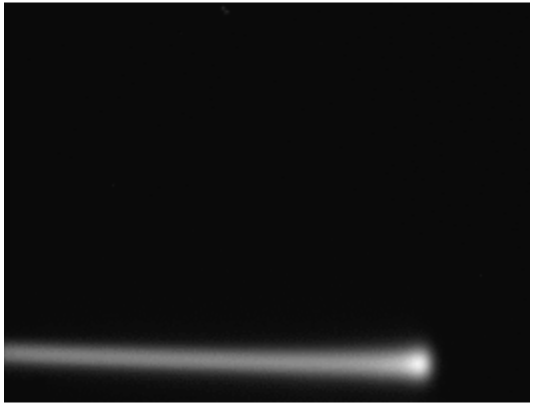

~~Conclusion~~ - Further Work

- **Trigger**
  - A more sensitive solution
  - Scanning is fast!
- **Scintillator**
  - Higher light output
  - Smaller form factor
- **Camera**
  - Faster acquisition
  - Wider FOV?

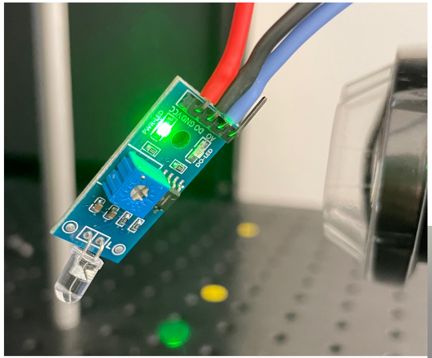

Acknowledgment

Dr. Charles-Antoine Collins Fekete
Dr. Mikaël Simard

Vasilis Rompokos
Alison Toltz
Dr. Ka Wing (Savanna) Chung

Dr. Lennart Volz

Dr. Daniel Robertson

Prof. Sam Beddar

This work was supported by:
The Radiation Research Unit at the Cancer Research UK City of London Centre Award C7893/A28990